Available online at www.sciencedirect.com
SCIENCE DIRECT
Polymer 46 (2005) 4571–4583
polymer
www.elsevier.com/locate/polymer

Comparison of photo-oxidative degradation of polyamide 6,6 films stabilized with HALS and $CuCl_2 + KI$ mixtures

Pierfrancesco Cerruti[a,b,*], Marino Lavorgna[c], Cosimo Carfagna[a,b], Luigi Nicolais[a,c]

[a]*Dipartimento di Ingegneria dei Materiali e della Produzione, Università di Napoli Federico II, P. le Tecchio 80, 80125 Napoli, Italy*
[b]*CNR-Istituto di Chimica e Tecnologia dei Polimeri, Via Campi Flegrei 34, 80078 Pozzuoli (Na), Italy*
[c]*CNR-Istituto per i Materiali Compositi e Biomedici, P. le Tecchio 80, 80125 Napoli, Italy*

Received 1 February 2005; received in revised form 26 March 2005; accepted 26 March 2005
Available online 19 April 2005

Abstract

The photo-oxidative stability of polyamide 6,6 (PA 6,6) doped with a hindered amine light stabilizer (HALS) and a mixture of cupric chloride and potassium iodide was examined.

Several analytical techniques were employed, in order to evaluate the correlation between chemical modifications, morphology and mechanical properties of PA 6,6 films irradiated at $\lambda > 300$ nm, 90 °C, and 50% relative humidity.

Infrared spectroscopy showed a build-up of carbonyl absorption in the range 1700–1780 cm^{-1} due to primary and secondary photo-oxidation products. The increase in content of carbonyl groups was greatest in the case of the pure polymer, and it was also appreciable in the case of PA 6,6 stabilized with copper/KI system. On the other hand, the use of the HALS additive brought about a substantial increase in the amount of carboxylic acids formed.

The morphology of the samples was found to have an effect on the kinetics of the accumulation of carbonyls, and it was observed that at a later stage of exposure the crystalline phase was also involved in the oxidation process.

Tensile tests on films revealed a large reduction in ductility as a result of ageing for both neat polymer and HALS-doped polymer. Only a slight reduction in ductility was found for the polymer stabilized with the inorganic mixture.

This study evidenced that the mixture of $CuCl_2$ and KI has a far better long-term stabilizing efficiency in comparison with the HALS stabilizer.

Keywords: Polyamide photo-oxidation; HALS stabilizers; Copper chloride and potassium iodide

1. Introduction

Synthetic polyamides (PA's) are commonly used for fibre production or as engineering resins. Owing to their good barrier properties, PA's have recently been used in multi-layered films for food packaging. However, thermal and photo-oxidative degradation can lead to the deterioration of physical and mechanical properties. The activation energy of the degradation reactions involved is often quite low and a deterioration of properties can occur even at low temperatures.

It has been shown that degradation mechanisms of thermal and photochemical oxidation are identical, except for the initiation step of the oxidation reaction [1,2].

Polyamide thermal oxidation occurs predominantly through the homolytic scission of carbon–hydrogen bonds of the methylene groups close to the nitrogen of amide group –CONH–CH_2– [3,4].

In the case of photo-oxidation, radiation with wavelength lower than 290 nm can initiate the oxidation of polyamides by direct cleavage of the C–N bond, which is the weakest bond in the polyamide chains [5,6]. In solar light, photochemical oxidation occurs if the polymer contains chromophores able to absorb radiation with wavelength longer than 290 nm. Although solar radiation does not possess sufficient energy to cause direct homolytic scission of the C–N bonds, the light

* Corresponding author. Address: Department of Materials and Production Engineering, University of Naples, Piazzale Tecchio, 80, 80125 Napoli, Italy. Tel.: +39 81 7682510; fax: +39 81 7682404.
E-mail address: cerruti@unina.it (P. Cerruti).

0032-3861/$ - see front matter © 2005 Elsevier Ltd. All rights reserved.
doi:10.1016/j.polymer.2005.03.065

absorption can favor homolytic scission of the carbon–hydrogen bond, due to impurities, such as catalyst residues, metal ions, and carbonyl or peroxide species formed during high temperature processing [7,8]. The decomposition of hydroperoxides formed during oxidation has a key role in initiating branching reactions during prolonged oxidation [9,10]. Very recently, it has been pointed out that Norrish I and Norrish II chain-cleavage reactions could also take place in the photo-oxidation process of nylon 6,6 [11].

In order to extend their longevity or to improve their recyclability, polyamides have to be stabilised with antioxidants that can withstand high processing temperatures (above 250 °C). Such severe processing conditions, however, may reduce the stabilizing efficiency of conventional antioxidants, like sterically hindered phenols, due to their thermal decomposition [12].

Secondary aromatic amines are efficient stabilizers against the oxidation reactions in polyamides, but their use can lead to discolorations with exposures to heat and oxygen [13].

Hindered amine light stabilizers (HALS) have opened new possibilities in the field of stabilization against photo-oxidation of synthetic polymers and polyamides as well. Within polymer matrix, they are readily converted to nitroxyl radicals that act as efficient scavengers of alkyl radicals [14].

Metal salts capable of forming coordination complexes with amide groups can affect the thermal and thermo-oxidative stability of polyamides [15–17]. Some studies on thermo-oxidative behavior of polyamide 6,6 (PA 6,6) containing different combinations of metal salts have shown that copper salts Cu(I) and Cu(II), especially when combined with iodides, are able to stabilize PA 6,6 [18–21] against thermal oxidation in a very efficient manner.

The main reaction pathways of the $CuCl_2$ activity on polyamide consist of a reaction sequence in which polymer and peroxy radicals are converted in non-reactive ionic species. Iodides can take part in the non-radical, reductive decomposition of hydroperoxides [18,22,23].

It is not known whether such a mechanism operates also for the stabilization of PA's against photo-oxidative degradation.

In this paper, we report the results of photo-oxidation experiments performed in air on PA 6,6 containing a mixture of copper chloride and potassium iodide in order to determine whether metal salts are able to stabilize polyamides against photo-oxidative degradation. The study includes also a comparison of their relative efficiencies with respect to the case of HALS.

2. Experimental

2.1. Materials

Unstabilized polyamide 6,6 containing less than 0.5% weight of residual oligomers (Radilon A), was kindly supplied by Radicinovacips SpA (Italy). This polymer has $\bar{M}_n = 17,500$ g/mol (as specified by the supplier), and the concentrations of terminal amino and carboxyl groups are, respectively, 46 and 75 meq/kg. The metal salts used to prepare the stabilized polyamide included $CuCl_2$ (98%) and KI (99%), purchased from Aldrich. The HALS was poly((6-((1,1,3,3-tetramethylbutyl)amino)-*s*-triazine-2,4diyl)((2,2,6,6-tetramethyl-4-piperidinyl)imino)hexamethylene((2,2,6,6-tetramethyl-4-piperidinyl)imino)) (Lowilite 94®), kindly supplied by Great Lakes Manufacturing Italy. All materials were used as received.

2.2. Polyamide samples preparation

Doped polymer samples were prepared by manually mixing polymer granules with a given amount of additive dissolved in water ($CuCl_2$/KI) or acetone (Lowilite 94®) (e.g. 100 mg $CuCl_2$ + 500 mg KI in 10 ml of solvent per 500 g of pure polymer). The solvent was then allowed to evaporate and the resulting mixtures were vacuum dried 24 h at 100 °C. Polymer films were prepared by extruding the mixtures in a counter-rotating, twin-screw extruder Haake, model CTW 100 fitted with a rod die, with the screws running at 40 rpm. The extruder temperature profile was 260, 275, 265, and 255 °C. The extrudate was then chill rolled at a temperature of 15 °C, in order to obtain films with 200 μm average thickness. Three different polyamide formulations were prepared, respectively, neat PA 6,6, PA 6,6 doped with 1000 ppm of Lowilite 94®, PA 6,6 doped with 200 ppm of $CuCl_2$ and 1000 ppm of KI [1,24–27].

2.3. Sample aging

Polymer films were subjected to photo-oxidative degradation at 90 °C and 50% relative humidity (RH) up to 528 h in a Angelantoni environmental chamber, model CH 250. Samples were irradiated using a Xenon lamp filtered with a borosilicate glass cutting off wavelengths lower than 300 nm. The irradiation power of the lamp was 800 W m^{-2}.

Aged samples were collected at different periods of exposure and subjected to chemical analysis and morphological examination, as well as being subjected to mechanical tests.

2.4. Experimental techniques

2.4.1. Differential scanning calorimetry (DSC)

Calorimetric analysis was performed under nitrogen flow using a DuPont DSC 2910, coupled with a thermal analyzer TA 2100, at a heating rate of 10 °C min^{-1}. The samples, weighing 4.0 ± 1 mg, were placed in crimped, non-hermetic aluminium pans.

The melting temperature and enthalpy were determined from the thermogram produced in the heating scan.

2.4.2. Wide angle X-ray diffraction (WAXD)

X-ray diffraction experiments were performed using a

Philips PW 1710 diffractometer with a rotating anode generator and a wide-angle power goniometer. The radiation was Cu K_α not filtered, with 40 kV voltage and 20 mA intensity. The scan rate was $1° \, min^{-1}$, over a diffraction angle 2θ ranging between 5 and 60°.

2.4.3. Fourier transform infrared spectroscopy (ATR-FTIR)

A diamond crystal Avatar Durascope ATR apparatus mounted on a Nicolet Nexus FTIR spectrometer was used. Spectra were recorded as an average of 32 scans in the range 4000–400 cm^{-1}. ATR corrections were performed using the Nicolet Omnic 5.2 software. The carbonyl stretching region (1800–1690 cm^{-1}) was deconvoluted using the Origin 6.1 software program, assuming Lorentzian bandshapes.

2.4.4. Mechanical properties

Tensile tests were performed using an Instron model 4204 dynamometer equipped with a 1 kN load cell. The results were evaluated by using the Instron Series IX software. The tests were performed at 23 ± 2 °C, 45 ± 5% RH with a 10 mm min^{-1} clamp separation rate.

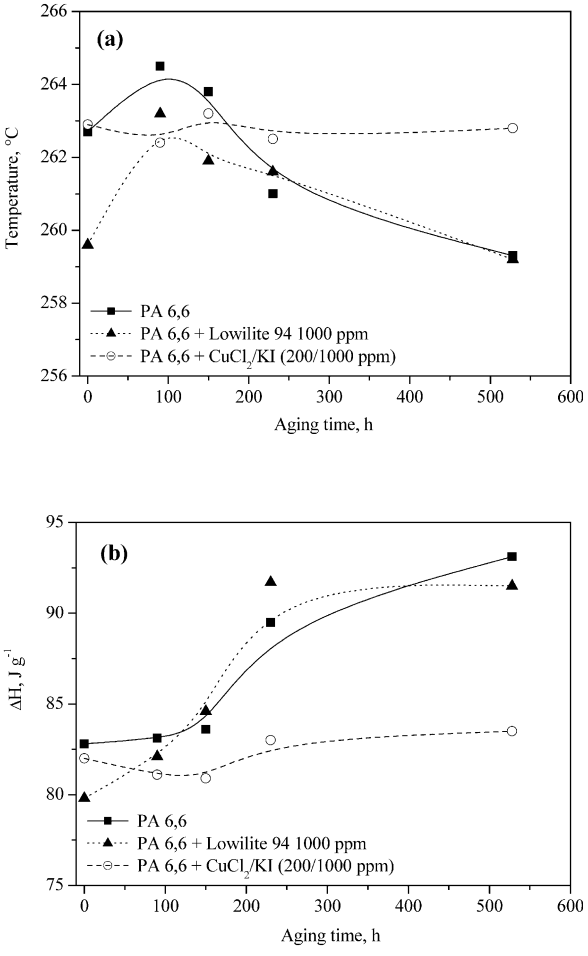

Fig. 1. Effects of photo-oxidation on (a) melting temperature and (b) melting enthalpy of neat and doped PA 6,6.

The test specimens were prepared according to ASTM D 882-02 standard test method, and they were conditioned prior to testing at 50% RH for at least 4 days in a desiccator containing a saturated $CaNO_3$ solution. Five specimens were used for each formulation.

2.4.5. Scanning electron microscopy (SEM)

Fracture surfaces of samples subjected to tensile tests were observed by a Leica S 440 scanning electron microscope. Samples were metallized before the observation with a gold–platinum mixture by means of a SC 500 emiscope.

3. Results and discussion

3.1. Differential scanning calorimetry (DSC) analysis

The effect of the irradiation of the different samples on the thermal properties is shown in Fig. 1 in terms of change in (a) melting temperature (T_m) and (b) melting enthalpy (ΔH) with ageing time. The data refer to the first heating run. The second heating cycle always results in a double peak in the melting region, due to re-crystallization processes in the DSC [28,29].

In the case of the pristine polymer and the HALS-doped polymer, prolonged exposure times cause a decrease of the melting temperature (Fig. 1(a)) and an increase of the melting enthalpy (Fig. 1(b)). Changes of melting temperature and enthalpy are difficult to predict, as they result from the occurrence of different simultaneous processes.

Short irradiation periods (up to 144 h) cause an increase in the melting temperature, which is more pronounced in the case of pristine and HALS-doped polymer.

At short irradiation times, a small increase in the melting enthalpy was observed for the HALS-doped polymer.

Long irradiation times, on the other hand, cause a significant reduction in melting temperature, accompanied by an increase of melting enthalpy, both for pure and HALS-doped PA 6,6. Under the same conditions, only minor changes of melting point and enthalpy are observed for the $CuCl_2$/KI-doped polymer.

The initial increase in T_m and melting enthalpy may be related to thermal annealing of the polymer, which improves the degree of perfection of the crystals and favors crystalline phase aggregation [30,31].

Chain scission results from the oxidation reactions as prolonged irradiation is carried out in the presence of oxygen. Photo-oxidation preferentially occurs in the amorphous region since this phase has higher oxygen permeability. The entangled tie-molecules are released as a result of chain scission and their rearrangement increases the overall crystallinity, as detected by DSC for both neat and HALS-doped PA 6,6.

However, the observed decrease in melting temperature peak indicates that the degradation affects also the

crystalline region [32]. In other words, the oxidative degradation can spread out to the tie molecules connecting the crystallites and the chain folds at crystal surfaces, causing cleavage of chains from the crystal surface [33,34]. The formation of less-ordered crystallites with an increased surface energy [35] results in a decrease of melting temperature.

The presence of $CuCl_2$ and KI brings about a slow-down in the rate of oxidative chain scission, as is confirmed by the observation of insignificant changes in melting temperature and enthalpy. Unchanged values of melting temperature also indicate that the crystalline phase of the polymer is not affected by any oxidative degradation reactions even after 500 h of exposure.

The presence of the HALS stabilizer, on the other hand, does not seem to provide an appreciable stabilization, since the changes of melting temperature and enthalpy are very similar to those observed for pure polymer. This may be related to the chemical structure of the stabilizer, which contains both piperidine and triazine moieties. The mechanism of triazine stabilization consists of the absorption of UV radiation and its dissipation as a radiation of a different wavelength. Besides having a very high absorption capacity, these compounds must be intrinsically very light stable, in order to avoid their photo-degradation [36,37].

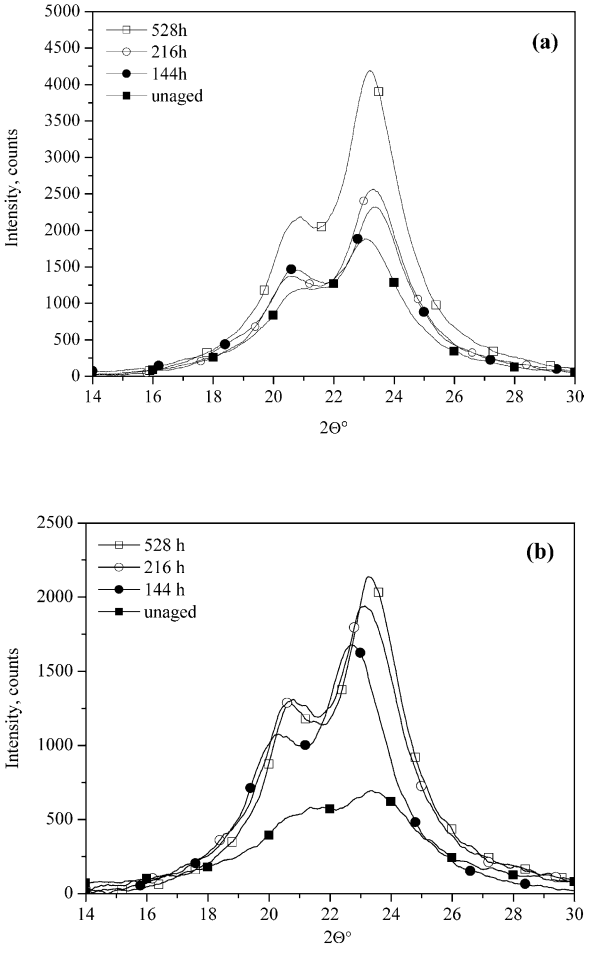

Fig. 2. Effect of photo-oxidation on X-ray diffraction patterns of (a) neat and (b) HALS-doped PA 6,6.

3.2. Wide angle X-ray diffraction (WAXD) analysis

The morphological changes resulting from aging for the different formulation samples were analyzed by wide-angle X-ray diffraction (WAXD). The X-ray diffraction patterns of both neat and HALS-doped polymers during irradiation are shown in Fig. 2(a) and (b), respectively. Two peaks are present at $2\theta = 20.5°$ and $2\theta = 23°$, respectively, due to 100 and 010 reflexes of the PA 6,6 α crystalline form. Their positions do not change with the time of exposure, whereas their intensities are markedly affected.

The diffraction intensity of the unaged HALS-doped PA 6,6 is considerably lower than that of the unaged neat polymer. This suggests that there is a lower level of surface crystallinity for the HALS-doped polymer. Furthermore, the diffraction spectra of PA 6,6 show a constant buildup of the diffraction intensity over the entire irradiation period, whilst the HALS-stabilized polymer shows that the intensity increases up to a maximum which occurs at 216 h of exposure.

WAXD data confirm the results obtained by DSC, however, it is worth noting that DSC measures the overall level of crystallinity (bulk polymer), whereas X-ray diffraction probes only the sample surface. Thus, for neat PA 6,6, the DSC analysis shows only a slight increase of crystallinity occurring in between 216 and 528 h, whereas over the same period, the XRD characterization indicates that there has been an appreciable surface crystallization. This is due to the direct oxidation of amorphous phase on the surface. The scission of the tie-molecules in the amorphous phase is able to cause the recrystallization of hindered chain segments [38].

The diffraction intensity values of the stabilized PA 6,6 are markedly lower than those of neat polymer at each aging time, which suggest that the presence of the organic stabilizer inhibits post-crystallization caused by thermal annealing and reorganization of the cleaved chains. This leads to higher oxygen permeability, and to a greater consumption of the organic stabilizer through oxidative degradation.

The X-ray diffraction patterns of $CuCl_2$/KI-doped polymer show only very small intensity changes over the aging period and, therefore, are not shown.

3.3. FTIR analysis of the photo-oxidized films

3.3.1. FTIR spectra of pure and doped PA 6,6

Infrared spectra of the PA 6,6 samples subjected to photo-oxidation at 90 °C show an increase of absorption intensity in the range 1780–1700 cm^{-1} during the exposure. These changes are due to the formation of carbonyl groups, which are accumulated in the polymer chains. Fig. 3 shows

the ATR-FTIR spectra of PA 6,6 in the carbonyl range at different times of exposure.

Some absorption bands, due to different species formed during aging, can be observed at 1760, 1735, 1725, 1710 cm^{-1}.

The peak at 1735 cm^{-1} is also detectable in the untreated polymer pellet prior to the preparation of samples. This absorption has been related to the presence of cyclopentanone derivatives by Soto-Valdez et al. [39]. They have observed the formation of cyclopentanone and 2-ethylcyclopentanone during thermal degradation of polyamide 6,6 under inert atmosphere. The aging conditions used were very similar to those found during polymerization and processing of polyamides. Furthermore, Groning et al. confirmed that these species are formed during the preparation of the samples, and their content tends to decrease during thermo-oxidation processes [40,41]. Fig. 3 shows that the 1735 cm^{-1} absorption markedly increases up to 96 h aging, and it remains practically constant thereafter up to 408 h.

This experimental evidence can be rationalized by taking into account the overall oxidation process of polyamides according to the scheme proposed by Tang et al. [42] (Scheme 1).

The initiation reactions are associated with the presence of impurities or defects within polymer chains. The oxidation attack in the polyamide chains occurs at the methylene groups close to the nitrogen of amido group –CONH–CH_2–, and it leads to the formation of hydroperoxides. The latter are unstable at temperatures above 60 °C. Their decomposition may cause the formation of alkoxy radicals, which may further accelerate the propagation reactions by branching the oxidation chain and imide groups, which are both unstable. This finally leads to the formation of more stable secondary oxidation products, such as aldehydes and carboxylic acids, especially after prolonged exposure. Imides present a characteristic absorption peak at 1735 cm^{-1}. The associated kinetics is complex, but it is reasonable to assume that imides can reach a steady state concentration within the polymer matrix. Consequently, the peak observed at 1735 cm^{-1} could result by the overlapping contributions from both cyclic ketones, whose content decreases over aging, and imides, which remain constant after some time.

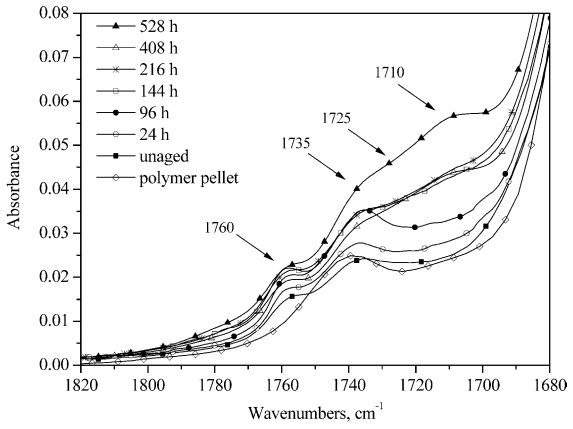

Fig. 3. Evolution of the carbonyl groups in the infrared spectra of PA 6,6 during photo-oxidation.

This mechanism can be also used to explain the 1760 cm^{-1} absorption peak, which results from species formed in the polymer just after the sample preparation, and increases only slightly during aging. This behavior is associated with the presence of highly stable secondary oxidation product. Philippart et al. [43] have attributed the absorption at 1755 cm^{-1} in polypropylene to isolated carboxylic acids, whose concentration remained constant even after photolysis reactions. It is possible that carboxylic acids formed within polymer bulk can exist as isolated species in equilibrium with dimeric acids (which absorb at 1710 cm^{-1}) due to their low mobility.

While the broad band ranging between 1730 and 1700 cm^{-1} increases overall during degradation, a steady absorption is observed between 144 and 408 h of exposure. This band is also due to the overlap of single species absorption, such as saturated aldehydes (at 1725 cm^{-1}), dimeric carboxylic acids (at 1710 cm^{-1}), and α,β-unsatured carbonyls (at 1700 cm^{-1}) [44,45]. The kinetics of the formation and accumulation of each species are different. Acids are formed as stable products, mainly in hydrogen-bonded associated form. Their concentration steadily increases due to the oxidation of intermediate oxidation products (aldehydes, imines), and to the hydrolysis of amide groups (Fig. 3 and Scheme 1). Aldehydes are produced during thermal and photolytic cleavage of the amide bonds [46], and as decomposition products of imides. However, they can be converted into carboxylic acids and α,β-unsaturated carbonyls [6,47,48].

Figs. 4 and 5 show the infrared spectra carbonyl region of the PA 6,6 containing HALS and the $CuCl_2$/KI mixture, respectively.

Fig. 4 shows that the presence of HALS inhibits the formation of isolated carboxylic acids at 1760 cm^{-1} up to 96 h. Thereafter, the absorbance intensity is comparable to that for the pure polymer. For the $CuCl_2$/KI-doped polymer, on the other hand, the absorption intensity is markedly lower even at long exposure, confirming the efficient level of stabilization conferred to PA 6,6 (Fig. 5).

According to Cerruti et al. [18], the main reaction pathways of the $CuCl_2$/KI effect on polyamide PH may consist of the following redox mechanism:

$$Cu^{2+} + P \rightarrow Cu^{+} + P^{+}$$

$$Cu^{+} + PO_2 \rightarrow Cu^{2+} + PO_2^{-}$$

KI participates in the non-radical decomposition of hydroperoxides. Iodide anions will react with hydroperoxides in a non-radical way as follows:

$$2POOH + 2I^{-} + 2H^{+} \rightarrow I_2 + 2POH + 2H_2O$$

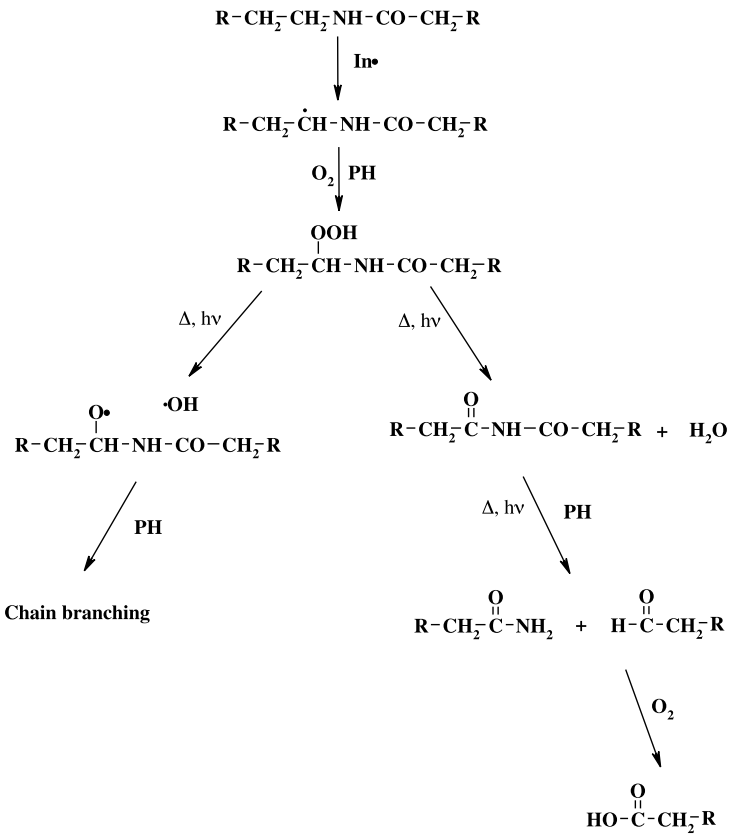

Scheme 1. Hydroperoxide decomposition mechanism for PA 6,6 photo-oxidation.

while elementary iodine may enter the reaction with Cu^+ ions:

$$Cu^+ + I_2 + 2H_2O \rightarrow Cu(OH)_2 + 2I^- + 2H^+$$

According to the above reactions, the $CuCl_2$/KI mixture may catalyze the non-radical decomposition of peroxides and hydroperoxides, inhibiting the propagation stages of the kinetic oxidative chain. This results ultimately in polymer stabilization. Furthermore, strong interactions between polymer amide groups and electron-attracting metal cations (which causes an electron displacement toward the metal center) reduce the reactivity of methylene groups adjacent to the amidic nitrogen. This leads to a retardation in hydroperoxide formation, as already observed in the case of polyamides and poly(ethylene oxide) [49,50].

Further insights about the physico–chemical processes related to the oxidative degradation of PA 6,6 can be obtained from the plots showing the increase of the overall carbonyls in the range 1695–1800 cm^{-1} (Fig. 6).

Both pure polyamide and the polymer doped with

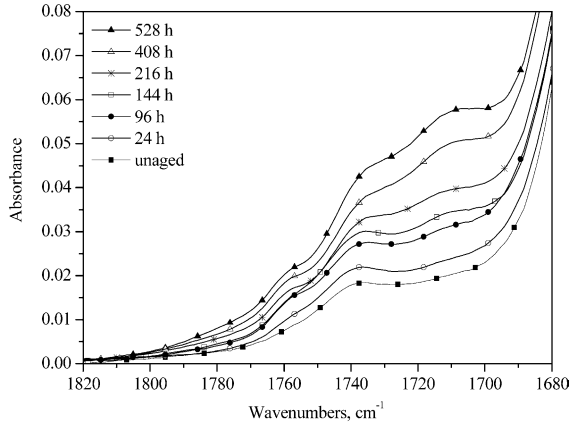

Fig. 4. Evolution of the carbonyl groups in the infrared spectra of HALS-doped PA 6,6 during photo-oxidation.

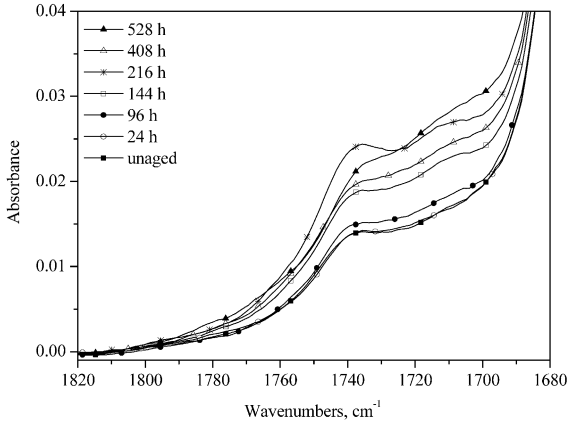

Fig. 5. Evolution of the carbonyl groups in the infrared spectra of $CuCl_2$/KI doped PA 6,6 during photo-oxidation.

$CuCl_2$/KI mixture show three kinetic stages of the carbonyl evolution. First, the increase in absorption intensity is observed up to approximately, 200 h, then a constant level of carbonyls is observed in the next 200 h, and finally the absorption intensity rises again in the final stage. The HALS-doped polymer, on the other hand, shows a constant increase in carbonyl absorption. In this case, the trend is similar to that already reported in the literature for the photo-oxidation of polyamides [32,45].

The different behavior of the HALS-doped polymer relative to the pure polyamide can be explained by taking into account the morphology of the samples. It is known that the morphology can play a key role in determining the rate of oxidation of polyamides [51]. Gijsman compared the thermo-oxidative degradation of PA 4,6 and PA 6,6. Although from chemical structure considerations PA 4,6 was expected to be less stable than PA 6,6, its half-life tensile strength was found to be double that observed with PA 6,6 [52]. This was explained in terms of inhibited diffusion of oxygen into the polymer matrix, due to higher crystallinity and density of the amorphous phase of PA 4,6. This observation can also help to explain the kinetic curve of the carbonyl groups in the case of the PA containing the HALS stabilizer. Oxidative degradation can only take place in the less-ordered domains of the polymer, because of the impermeability of the crystalline phase to the oxygen. As already observed in the WAXD experiments (Section 3.2), the surface crystallinity is lowest for the PA containing the organic stabilizer (HALS). It can be deduced, therefore, that the increased oxidizable fraction accounts for the linear build-up of carbonyls. Crystallinity differences can also explain the three-stage kinetic curves observed for neat and $CuCl_2$/KI-doped polyamide. In the first stage, the amorphous phase undergoes oxidation due to the fast diffusion of oxygen, as it is witnessed by the increase of carbonyl absorption and crystallinity. In a second stage, the photo-oxidation process is slowed down due to the large reduction in the fraction of amorphous phase present. In the final stage, even the crystalline phase can be degraded [53,54], as

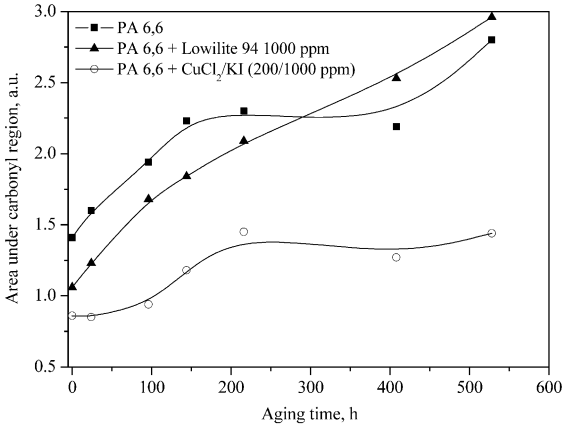

Fig. 6. Increase of the carbonyl area from infrared spectra of neat, HALS-doped and $CuCl_2$/KI-doped PA 6,6 over the photo-aging period.

it is confirmed by the increase of the carbonyl absorption after long exposure, and by the invariant melting enthalpies, which are directly related to the reduction in the extent of crystallization resulting from the cleaved chains.

3.3.2. Deconvolution of the FTIR spectra

In order to monitor the evolution of the various carbonyl compounds during the photo-oxidative degradation, deconvolution of the carbonyl envelope between 1800 and 1690 cm^{-1} was carried out, using six peaks. The analytical procedure was performed by using Microcal Origin 6.0 software. The number and the absorption values of the peaks were set using second derivative of the spectra. The identification of each peak is shown in Table 1 [31,43].

The peaks were fitted by Lorentzian functions. A backwards procedure was followed. First, the most structured spectra (corresponding to the longest times of exposure) were fitted, leaving free all the parameters (peak center wavenumber and half-height width). Subsequently, the fitting procedure was improved by setting parameter constraints. Then, spectra related to shorter times of exposure were deconvoluted, by using the refined parameters.

Fig. 7 shows the results of peak deconvolution in the case of PA 6,6 after 528 h of exposure. The correspondence between the experimental spectrum and the curve calculated as a sum of single peaks is satisfactory.

Changes of the area of single peaks during the aging of PA 6,6 and PA 6,6 doped with the HALS are shown in Fig. 8(a) and (b), respectively.

The deconvolution procedure of $CuCl_2$/KI-doped PA 6,6 is not shown, as the small carbonyl area did not give very reliable results.

Both figures show that, with the exception of the peak at 1735 cm^{-1}, the amount of all carbonyl species increases upon aging. As previously pointed out for the polymer control, this absorption is due to cyclic ketones and imides. The increase in peak area occurring in the early oxidation stages is due to the rapid formation of imides, whilst the subsequent decrease could be explained taking into account the decomposition of ketones during the photo-oxidation.

In the case of the HALS-stabilized polymer this band shows a more intense absorption, which could be due to products formed by the reaction between the polymer and the stabilizer itself. Low molecular weight hydroxylamines

Table 1
Assignment of the carbonyl absorptions used to perform the deconvolution procedure

Wavenumbers (cm^{-1})	Species
1635	Amides
1700	Conjugated carbonyls
1710	Associated carboxylic acids
1725	Aldehydes
1735	Imides and cyclic ketones
1760	Isolated carboxylic acids

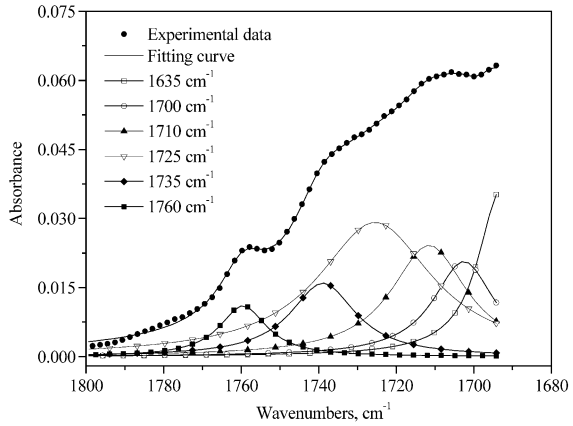

Fig. 7. Deconvolution of infrared spectra for carbonyl groups for a PA 6,6 sample subjected to 528 h photo-oxidation.

and nitroso-containing macroradicals, which absorb at 1735 cm^{-1}, can be produced on the basis of the HALS stabilization mechanism [55].

In the case of neat polyamide, the aldehyde groups show the largest changes. In the first stage (up to 144 h), aldehydes are quickly formed during the oxidation of the amorphous phase, becoming the prevailing species. Subsequently (up to 408 h), their concentration remains constant, because of depletion of the amorphous phase caused by thermal annealing and recrystallization of the oxidized chains. Aldehydes are also transformed into carboxylic acids and α,β-unsatured compounds [8,44,47,48]. Finally, an increase in aldehyde groups takes place again, due to oxidation of the crystalline phase.

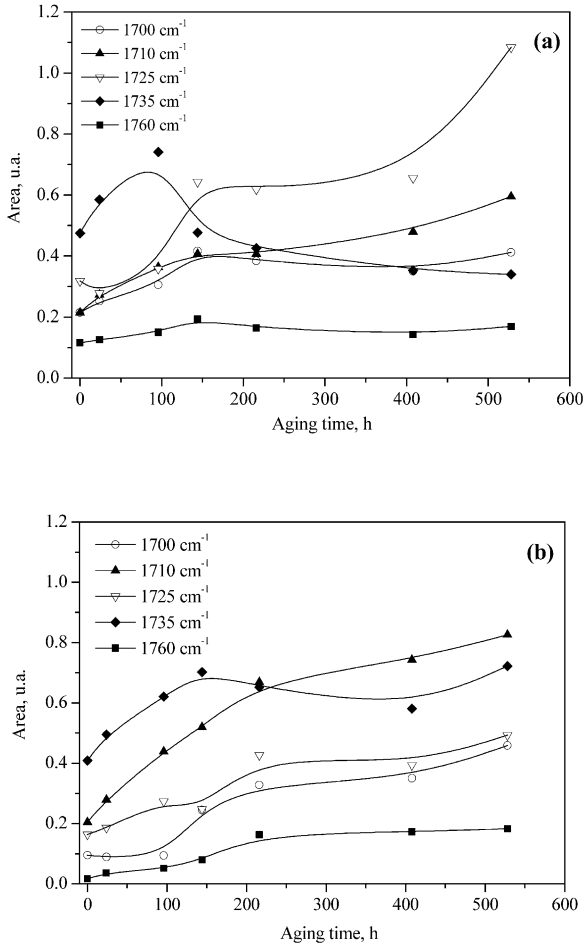

Fig. 8. Area changes of the deconvoluted carbonyl peaks of (a) neat and (b) HALS-doped PA 6,6 as a function of aging time.

Although the HALS-doped polymer displays a greater amount of oxidizable phase (as evidenced by DSC and WAXD analysis) the aldehyde concentration in this system is lower than that observed for the neat PA 6,6 (Fig. 8(b)).

Furthermore, in the case of the HALS-doped polymer, carboxylic acids show the greatest rates of formation, and they are more abundant with respect to aldehydes.

According to the generally accepted interpretation of the stabilization mechanism of HALS, this experimental result can be rationalized if the formation of acyl radicals is assumed to play an important role in the initiation reaction of the PA 6,6 photo-oxidation process.

Accordingly, the oxidation of acyl radicals would lead to acylperoxy radicals that are converted very efficiently to carboxylic acid by reacting with hindered amines or with aminoethers formed in the reaction between polymer radicals and nitroxyl radicals (Scheme 2) [56,57].

Acyl radicals can be formed through Norrish I type reactions, involving the cleavage of the C–C bond formed between carbonyl and methylene groups [11].

Another source of acyl radicals is the photolysis of the C–N bonds. In fact, the triazine groups present in the structure of the organic additive could also act as a photosensitizer for PA 6,6, facilitating the cleavage of the C–N link [11].

Finally, it is noteworthy that the formation of conjugate compounds (at 1700 cm^{-1}) shows an appreciable induction period in the case of the HALS-stabilized polymer, and their content increases only after extensive oxidation, even though their amount seems to be lower than that of aldehydes and acids.

3.4. Tensile tests and scanning electron microscopy (SEM) observation

Tensile tests performed on neat and HALS-doped PA 6,6 are reported in Fig. 9. The curves refer to unaged and 528 h aged samples.

For both formulations a great reduction in ductility is observed after aging. The polymer stabilized with the mixture $CuCl_2$/KI (Fig. 10) shows only a slight reduction in the strain at break, while the tensile strength remains almost constant. This is a manifestation of the efficient stabilization achieved against photo-oxidation.

The decrease of the molecular weight of the polyamide due to oxidation and hydrolysis of the amide bond, and the post-crystallization of amorphous phase and cleaved chains,

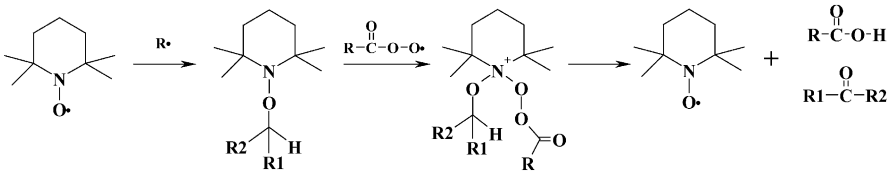

Scheme 2. Carboxylic acids formation through the reaction between acylperoxy radicals and HALS aminoethers.

are the main factors causing the observed changes in tensile properties.

Although hydrolysis causes a reduction of molecular weight, Tsvankina et al. have shown that the molecular weight of PA 6,10 aged 20 days in air at 90 °C and 75% relative humidity, decreases only 10% more than that of the same polymer subjected to the equivalent ageing procedure in a dry atmosphere [58]. Furthermore, given the low additive concentrations we have used in the present study, it can be concluded that all the samples should have the same susceptibility to hydrolysis.

It is noted that aging brings about a change in fracture mechanism from ductile to brittle. This behavior is observed for the case of the 528 h aged neat and HALS-doped polymers.

The above conclusion is also supported by the SEM analysis of the fracture surfaces of samples subjected to tensile tests (Fig. 11). Before aging, polymer fibrils are formed as a result of a ductile fracture mechanism for all the formulations.

The occurrence of degradation has a marked effect on the fracture surfaces. The unstabilized aged polymer shows (Fig. 11(b)) a smooth surface, in which clear fracture planes are observed. A similar behavior is observed in the case of HALS-doped polyamide (Fig. 11(c) and (d)).

In the case of $CuCl_2$/KI-doped PA6,6, on the other hand,

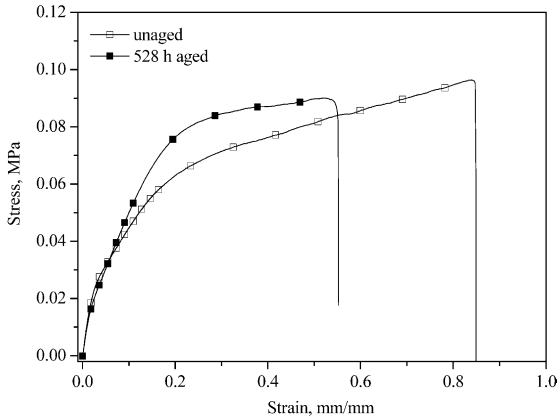

Fig. 10. Stress–strain curves for $CuCl_2$/KI-doped PA 6,6 before and after 528 h photo-oxidation.

even after 528 h aging a considerable stretching of the polymer fibrils can be still observed (Fig. 11(f)), especially in the inner part of the sample. This behavior confirms that the presence of the inorganic phase leads to an effective stabilization, due to the reduction in the rate of photo-oxidation.

Changes of strain at break and tensile strength over the aging period are reported in Fig. 12(a) and (b), respectively.

According to these data, for short-time exposure the decrease in overall fracture energy (area under the curve) of

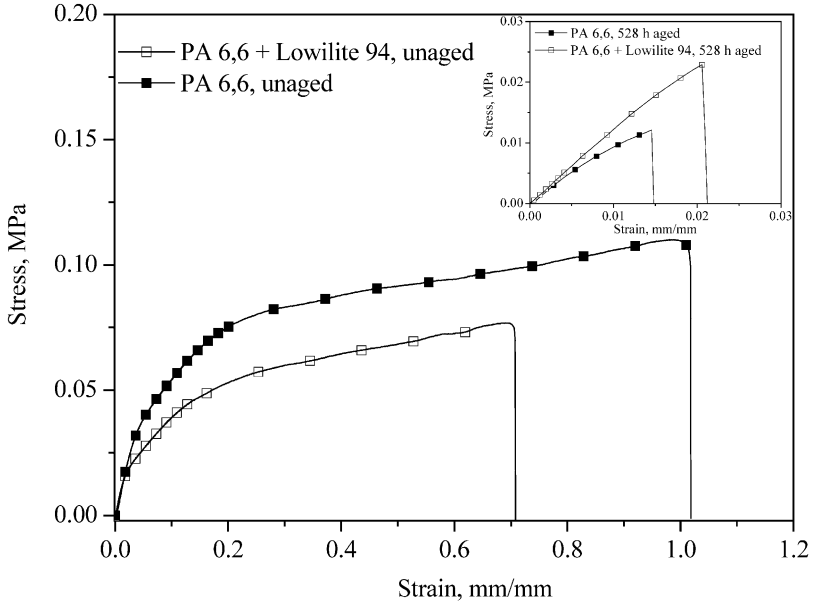

Fig. 9. Stress–strain curves of neat and HALS-doped PA 6,6 before and after 528 h photo-oxidation (figure inset).

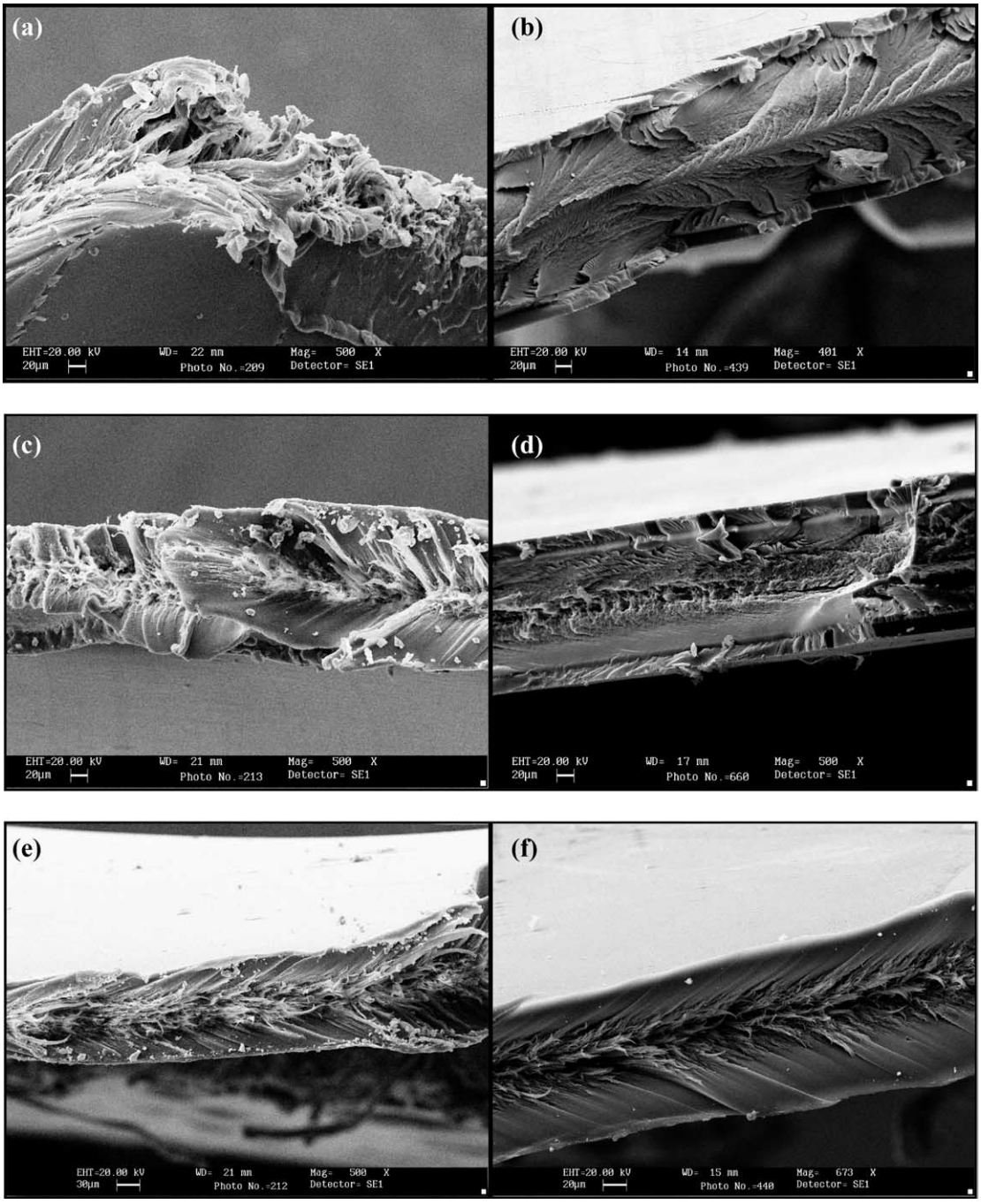

Fig. 11. SEM micrographs of fracture surfaces of failed tensile specimens for (a) unaged PA 6,6, (b) 528 h aged PA 6,6, (c) unaged HALS-doped PA 6,6, (d) 528 h aged HALS-doped PA 6,6, (e) unaged $CuCl_2$/KI-doped PA 6,6 and (f) 528 h aged $CuCl_2$/KI-doped PA 6,6.

the samples containing the HALS and the inorganic stabilizers is mainly due to the reduction of the elongation at break (Fig. 12(a)), as these samples do not show any appreciable reduction in tensile strength during the first 100 h of exposure (Fig. 12(b)). A reduction of both elongation at break and tensile strength is observed, on the other hand, in the case of the neat polyamide. Harding and McNulty showed that the tensile strength of non-reinforced polymers drastically drops when a critical value of the molecular weight of the polymer at the surface is reached [59].

From the results of our study it can be hypothesized that, for short-time exposure, in the case of the stabilized samples the effects of post-crystallization of the amorphous phase, due to thermal annealing, prevail over the molecular weight reduction due to oxidative degradation.

As for the neat polymer, thermal annealing is also accompanied by an appreciable reduction in molecular

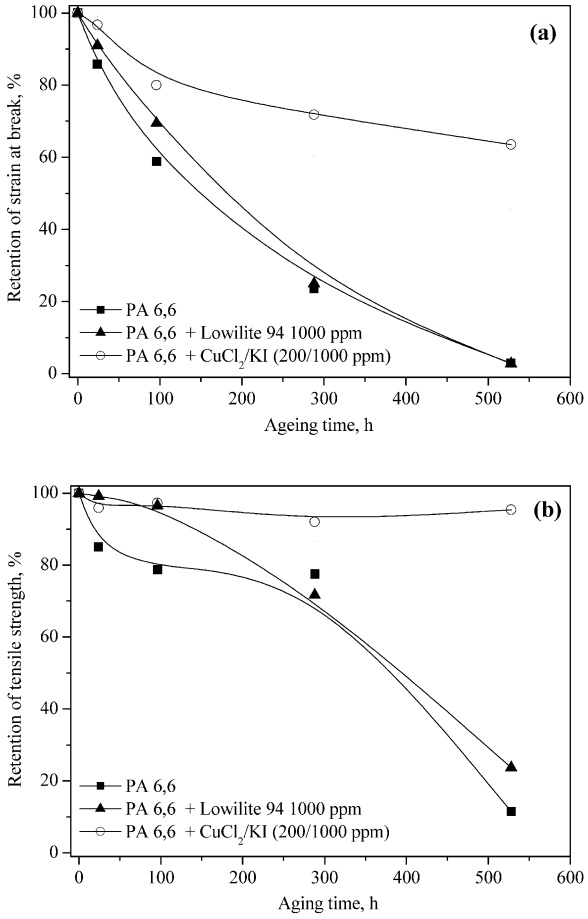

Fig. 12. Changes in (a) strain at break and (b) stress at break of neat, HALS-doped and $CuCl_2$/KI-doped PA 6,6 as a function of aging time.

weight due to thermal oxidation, as confirmed by the observed decrease in tensile strength [60].

At longer times, both the neat and the HALS-doped PA 6,6 show a dramatic drop in elongation at break and strength, as a result of oxidative degradation.

In particular, a marked decrease in tensile strength takes place even before 100 h of exposure for the case of the neat polymer, whereas the HALS is able to stabilize the polymer for up to 300 h. The constant tensile strength evidenced by $CuCl_2$/KI-doped polymer even at after 500 h aging suggests that there are only slight changes of molecular weight over the entire irradiation period.

4. Conclusions

In this paper, the stabilization against photo-oxidation provided by a HALS stabilizer and a $CuCl_2$/KI mixture in polyamide 6,6 films was studied.

DSC and X-ray diffraction results have shown that the photo-oxidative degradation of neat and HALS-doped PA 6,6 causes an increase in melting enthalpy and a decrease in melting temperature. This is due to both thermal annealing effects and reduction in molecular weight of polymer caused by the scission reactions in the amorphous phase. The presence of the HALS slows down crystallization of the polymer and increases the amount of the oxidizable amorphous phase, leading to a reduction in the efficiency of the organic stabilizer.

There is a good correlation between the results of tensile tests and FTIR spectroscopy data, which showed a build-up of carbonyl species in the range 1700–1780 cm^{-1}.

The kinetic profile of the carbonyl accumulation is markedly affected by the morphology of the samples, showing three distinct stages of carbonyl increase in the case of the neat polymer. This also confirms that at a later stage of exposure the crystalline phase can also be oxidized.

The deconvolution of the infrared spectra has shown that the presence of the HALS also leads to an increase in relative amounts of carboxylic acids formed. This indicates that besides hydroperoxide decomposition, Norrish I type reactions are involved in the initiation of the oxidation reaction. In fact, increased amounts of carboxylic acids are formed in presence of hindered amines through the oxidation of acylperoxy radicals produced by reaction of the atmospheric oxygen with acyl radicals.

The change observed indicate that copper/KI system have a far better long-term stabilizing efficiency in comparison with the HALS stabilizer. This is attributed to the non-radical decomposition of the polymer peroxides, favored by the $CuCl_2$/KI mixture, which prevents the occurrence of the oxidative propagation reactions during the aging process.

Acknowledgements

Mr Lucio Iadicicco is gratefully thanked for his valuable assistance in carrying out the photo-oxidation procedure. Thanks are addressed to Dr Aldo Filippi at Radicinovacips for very kind supplying the unstabilized polyamide 6,6.

References

[1] Ciaperoni A, Mula A. Chimica e Tecnologia delle Poliammidi. Pisa, Italy: Pacini editore; 2001 [chapter 2].
[2] Do CH, Pearce EM, Bulkin BJ, Reimschuessel HK. FT-IR spectroscopic study on the photo- and photooxidative degradation of nylons. J Polym Sci, Part A: Polym Chem 1987;25(8):2301–21.
[3] Do CH, Pearce EM, Bulkin BJ, Reimschuessel HK. FT-IR spectroscopic study on the thermal and thermal oxidative degradation of nylons. J Polym Sci, Part A: Polym Chem 1987;25(8):2409–24.
[4] Lánská B, Matisová-Rychlá L, Rychlý J. Stabilization of polyamides IV. Thermo-oxidation of hexano-6-lactam in the presence of alkali metal salts. Polym Degrad Stab 2005;87(2):361–73.
[5] Lemaire J, Arnaud R, Gardette JL. The role of hydroperoxides in photooxidation of polyolefins, polyamides and polyurethane elastomers. Pure Appl Chem 1983;55(10):1603–14.

[6] Allen NS. Thermal and photo-chemical oxidation of nylon 66. Some aspects of the importance of α,β-unsaturated carbonyl groups and hydroperoxides. Polym Degrad Stab 1984;8(1):55–62.
[7] Gijsman P, Meijers G, Vitarelli G. Comparison of the UV-degradation chemistry of polypropylene, polyethylene, polyamide 6 and polybutylene terephthalate. Polym Degrad Stab 1999;65(3):433–41.
[8] Lanska B. In: Puffr R, Kubanek V, editors. Lactam based polyamides, I. London: CRC press; 1991 [chapter 7].
[9] Roger A, Sallet D, Lemaire J. Photochemistry of aliphatic polyamides. 4. Mechanisms of photooxidation of polyamides 6, 11, and 12 at long wavelengths. Macromolecules 1986;19(3):579–84.
[10] Lánská B, Šebenda J. The effect of carboxylic and basic end-groups on the thermooxidation of hydrolytic polymers of lactams. Eur Polym J 1986;22(3):199–202.
[11] Carroccio S, Puglisi C, Montaudo G. MALDI investigation of the photooxidation of nylon-66. Macromolecules 2004;37:6037–49.
[12] Lánská B. Stabilization of polyamides. I. The efficiency of antioxidants in polyamide. Polym Degrad Stab 1996;53:89–98.
[13] Gugumus F. In: Gächter R, Muller H, editors. Plastics additives. 3rd ed. Munich: Hanser; 1990. p. 1–104.
[14] Bowry VW, Ingold KU. Kinetics of nitroxide radical trapping. 2. Structural effects. J Am Chem Soc 1992;114(13):4992–6.
[15] Dunn P, Samsom GF. The stress cracking of polyamides by metal salts. Part I. Metal halides. J Appl Polym Sci 1969;13:1641–55.
[16] Chao LC, Chang EP. Interaction of anhydrous ferric chloride with nylon 6. J Appl Polym Sci 1981;26:603–10.
[17] Siegmann A, Baraam Z. Nylon-6 containing metal halides II: tensile properties. Polym Eng Sci 1981;21(4):223–6.
[18] Cerruti P, Rychly J, Matisova-Rychla L, Carfagna C. Chemiluminescence from oxidation of polyamide 6,6 II. The effect of metal salts. Polym Degrad Stab 2004;84(2):199–206.
[19] Janssen K, Gijsman P, Tummers D. Mechanistic aspects of the stabilization of polyamides by combinations of metal and halogen salts. Polym Degrad Stab 1995;49(1):127–33.
[20] Allen NS, McKellar JF, Wilson D. Luminescence and degradation of nylon polymers II: quenching of fluorescent and phosphorescent species. J Photochem 1977;7:319–24.
[21] Broadbelt LJ, Klein MT, Dean BD, Andrews SM. Thermal degradation of aliphatic-aromatic polyamides: kinetics of *N,N′*-dihexylisophthalamiide neat and in presence of copper iodide. J Appl Polym Sci 1995;56(7):803–15.
[22] Mair RD, Graupner AJ. Determination of organic peroxides by iodine liberation procedures. Anal Chem 1964;36(1):194–204.
[23] Carlsson DJ, Lacoste J. A critical comparison of methods for hydroperoxide measurement in oxidized polyolefins. Polym Degrad Stab 1991;32(3):377–86.
[24] Paolino PR. Antioxidants. In: Lutz JT, editor. Thermoplatic polymer additives. Theory and practice. New York: Marcel Dekker; 1989. p. 15.
[25] Zweifel H. Plastics additives handbook. Munich: Hanser Publishers; 2001. p. 80.
[26] Allen NS, Edge M, Corrales T, Catalina F. Stabiliser interactions in the thermal and photooxidation of titanium dioxide pigmented polypropylene films. Polym Degrad Stab 1998;61:139–49.
[27] Malík J, Ligner G. Hindered amine light stabilizers: introduction. In: Pritchard G, editor. Plastic additives. An A–Z reference. London: Chapman & Hall; 1998. p. 357.
[28] Siegmann A, Baraam Z. Melting and crystallization of nylon 6 containing copper chloride. J Appl Polym Sci 1980;25(6):1137–43.
[29] Hybart FJ, Platt JD. The melting of 66 nylon: observations by differential thermal analysis. J Appl Polym Sci 1967;11:1449–60.
[30] Jain A, Vijayan K. Effect of thermal aging on nylon 6,6 fibres. J Mater Sci 2002;37(13):2623–33.
[31] Khabbaz F, Albertsson AC, Karlsson S. Chemical and morphological changes of environmentally degradable polyethylene films exposed to thermo-oxidation. Polym Degrad Stab 1999;63(1):127–38.
[32] Thanki PN, Singh RP. Photo-oxidative degradation of nylon 66 under accelerated weathering. Polymer 1998;39(25):6363–7.
[33] Oswald HJ, Turi A. Deterioration of polypropylene by oxidative degradation. Polym Eng Sci 1965;5(3):152–8.
[34] Ogier L, Rabello MS, White JR. Influence of morphology and surface preparation on the weatherability of polypropylene. J Mater Sci 1995; 30(9):2364–76.
[35] Eriksson PA, Boydell P, Eriksson K, Manson JAE, Albertsson AC. Effect of thermal-oxidative aging on mechanical, chemical, and thermal properties of recycled polyamide 66. J Appl Polym Sci 1997; 65(8):1619–30.
[36] Rytz G, Hilfiker R, Schmidt E, Schmitter A. Introduction to a new class of high-performance light stabilizers and the influence of light stabilizers structure on the polymer's life time. Angew Makromol Chem 1997;247:213–24.
[37] Zweifel H. Stabilization of polymeric materials. Heidelberg: Springer; 1997 [chapter 2].
[38] Billingham NC, Prentice P, Walker TJ. Some effects of morphology on oxidation and stabilization of polyolefins. J Polym Sci Polym Symp 1976;57:287–97.
[39] Soto-Valdez H, Gramshaw JW. Cyclopentanone and cyclopentanone derivatives as degradation products of polyamide 6,6. J Mater Sci Lett 2000;19(10):823–5.
[40] Groning M, Hakkarainen M. Headspace solid-phase microextraction—a tool for new insights into the long-term thermo-oxidation mechanism of polyamide 6.6. J Chromatogr A 2001;932(1–2):1–11.
[41] Groning M, Hakkarainen M. Headspace solid-phase microextraction with gas chromatography/mass spectrometry reveals a correlation between the degradation product pattern and changes in the mechanical properties during the thermooxidation of in-plant recycled polyamide 6,6. J Appl Polym Sci 2002;86(13):3396–407.
[42] Tang L, Sallet D, Lemaire J. Photochemistry of polyundecanamides. 1. Mechanisms of photooxidation at short and long wavelengths. Macromolecules 1982;15(5):1432–7.
[43] Philippart JL, Sinturel C, Arnaud R, Gardette JL. Influence of the exposure parameters on the mechanism of photooxidation of polypropylene. Polym Degrad Stab 1999;64(2):213–25.
[44] Fromageot D, Roger A, Lemaire J. Thermooxidation yellowing of aliphatic polyamides. Angew Makromol Chem 1989;170:71–85.
[45] Roger A, Sallet D, Lemaire J. Photochemistry of aliphatic polyamides. 3. Mechanisms of photooxidation of polyamides 6, 11, and 12 at short wavelength. Macromolecules 1985;18(9):1771–5.
[46] Sharkey WH, Mochel WE. Mechanism of the photooxidation of amides. J Am Chem Soc 1959;81:3000–5.
[47] Karstens T, Rossbach V. Thermooxidative degradation of polyamide 6 and 6,6. Kinetics of the formation and inhibition of UV/VIS-active chromophores. Makromol Chem 1989;190(12):3033–53.
[48] Marechal P, Legras R, Dekoninck JM. Postcondensation and oxidation processes in molten polyamide 6. J Polym Sci, Part A: Polym Chem 1993;31:2057–67.
[49] Khanna YP, Pearce EM. Aromatic polyamides. V. Substitution effect on thermal properties. J Appl Polym Sci 1982;27:2053–64.
[50] Costa L, Gad AM, Camino G, Cameron GG, Qureshi MY. Thermal and thermooxidative degradation of poly(ethylene oxide)-metal salt complexes. Macromolecules 1992;25:5512–8.
[51] Levchik SV, Weil ED, Lewin M. Thermal decomposition of aliphatic nylons. Polym Int 1999;48(7):532–57.
[52] Gijsman P, Tummers D, Janssen K. Differences and similarities in the thermooxidative degradation of polyamide 46 and 66. Polym Degrad Stab 1995;49(1):121–5.
[53] Eriksson PA, Boydell P, Eriksson K, Maanson JAE, Albertsson AC. Effect of thermal-oxidative aging on mechanical, chemical, and thermal properties of recycled polyamide 66. J Appl Polym Sci 1997; 65(8):1619–30.
[54] Thanki PN, Ramesh C, Singh RP. Photo-irradiation induced morphological changes in nylon 66. Polymer 2001;42(2):535–8.

[55] Delprat P, Duteurtre X, Gardette JL. Photooxidation of unstabilized and HALS-stabilized polyphasic ethylene–propylene polymers. Polym Degrad Stab 1995;50(1):1–12.
[56] Klemchuk PP, Gande ME. Stabilization mechanisms of hindered amines. Polym Degrad Stab 1988;22(3):241–74.
[57] Klemchuk PP, Gande ME, Cordola E. Hindered amine mechanisms. Part III. Investigations using isotopic labeling. Polym Degrad Stab 1990;27(1):65–74.
[58] Tsvankina AL, Dubovik PT, Neverov AN, Papkov VS. Thermal aging of poly(dodecaneamide) in wet atmosphere. Polym Sci USSR 1984; 26(2):423–31.
[59] Harding GW, MacNulty BJ. High temperature resistance and thermal degradation of polymers, SCI monograph, 13. London: SCI; 1961. p. 392.
[60] Pavlov NN, Kudryavtseva GA, Abramova IM, Vasil'eva VA, Zezina LA, Kazaryan LG. Structural and chemical changes in aliphatic polyamides during artificial aging. Polym Degrad Stab 1989;24(4):389–97.